Check for updates

ARTICLE

Mucosal-associated invariant T cells have therapeutic potential against ocular autoimmunity

Satoshi Yamana[1], Kensuke Shibata [1,2,3 ✉], Eiichi Hasegawa[1], Mitsuru Arima[1], Shotaro Shimokawa[1], Nobuyo Yawata[1], Atsunobu Takeda[1], Sho Yamasaki[3,4,5,6] and Koh-Hei Sonoda[1]

Autoimmune uveitis is a sight-threatening disease induced by pathogenic T cells that recognize retinal antigens; it is observed in disorders including Vogt–Koyanagi–Harada disease (VKH). The roles of specific T cell subsets and their therapeutic potential against autoimmune uveitis are not fully understood. Here we conducted multi-parametric single-cell protein quantification which shows that the frequency of CD161^{high}TRAV1-2^{+} mucosal-associated invariant T (MAIT) cells that recognize vitamin B2 metabolite-based antigens is decreased in relapsing VKH patients compared to individuals without active ocular inflammation. An experimental autoimmune uveitis (EAU) mouse model revealed that genetic depletion of MAIT cells reduced the expression of *interleukin* (*Il*) *22* and exacerbated retinal pathology. Reduced IL-22 levels were commonly observed in patients with relapsing VKH compared to individuals without active ocular inflammation. Both mouse and human MAIT cells produced IL-22 upon stimulation with their antigenic metabolite in vitro. An intravitreal administration of the antigenic metabolite into EAU mice induced retinal MAIT cell expansion and enhanced the expressions of *Il22*, as well as its downstream genes related to anti-inflammatory and neuroprotective effects, leading to an improvement in both retinal pathology and visual function. Taken together, we demonstrate that a metabolite-driven approach targeting MAIT cells has therapeutic potential against autoimmune uveitis.

INTRODUCTION
Autoimmune uveitis, including birdshot retinochoroidopathy, sarcoidosis, Behcet's disease and Vogt–Koyanagi–Harada disease (VKH), is a leading cause of uveitis and accounts for up to 10% of cases related to blindness in the United States[1]. Although the pathogenesis of autoimmune uveitis is not completely understood, T cell-mediated responses to ocular antigens such as S-antigens, interphotoreceptor retinoid-binding protein (IRBP), and recoverin have been frequently observed[2]. Animal models of autoimmune uveitis immunized with retinal antigens including retinal arrestin, IRBP, and recoverin, and a retinal antigen-specific T cell transfer experiment[3] recapitulate these symptoms. Thus, T cell-mediated autoimmune reactions to self-antigens in the eye have pathogenic roles in the development of the autoimmune eye diseases. Supporting this, particular haplotypes of human leukocyte antigens (HLA) that are responsible for T cell activation have been associated with different types of uveitis[3]. Although the contribution of retinal peptide-specific autoreactive T cells to the pathogenesis has been well documented, the protective roles of T cell subsets in autoimmune uveitis are relatively unclear.

VKH is a type of autoimmune uveitis that targets melanocyte-derived antigens such as tyrosinase, gp100 and melanoma-associated antigen peptides such as KU-MEL-1 in the eye[4]. The recognition of these antigens by T cells is involved in pathogenic responses to ocular melanocytes by direct cell killing activity and/or by promoting the production of autoantibodies[5,6]. VKH is observed more commonly in Hispanic and Asian populations[7,8] and accounts for up to 8.1% of autoimmune uveitis cases in Japan[9]. Steroid therapy has been used as a first-line treatment of VKH; however, ocular inflammations persist in approximately one-quarter of the patients after steroid therapy[10,11], possibly due to a faster tapering schedule and/or an inadequate dose of the steroid[12]. Alternative immunomodulatory approaches are thus required for patients with VKH.

Mucosal-associated invariant T (MAIT) cells are an innate-like T cell subset that harbors unique invariant TRAV1-TRAJ33^{+} chains paired with limited T cell receptor (TCR) β chains[13]. Through these receptors, MAIT cells recognize a microbial vitamin B2 precursor-derived metabolite, 5-(2-oxopropylideneamino)-6-D-ribitylami-nouracil (5-OP-RU)[14], which is presented by a monomorphic major histocompatibility complex class I-related gene protein (MR1). Upon recognition of the cognate antigen, MAIT cells secrete immunoregulatory molecules including IL-2, IL-17A, tumor necrosis factor-alpha (TNF-α), interferon-gamma (IFN-γ), granulocyte-macrophage colony-stimulating factor (GM-CSF), IL-10, IL-22 and granzyme B[13,15–17]. By producing such multifaceted cytokines, MAIT cells contribute to immunoregulation in various disease settings including infection, autoimmune disorders, and

[1]Department of Ophthalmology, Graduate School of Medical Sciences, Kyushu University, Fukuoka, Japan. [2]Department of Microbiology and Immunology, Graduate School of Medicine, Yamaguchi University, Yamaguchi, Japan. [3]Department of Molecular Immunology, Research Institute for Microbial Diseases, Osaka University, Osaka, Japan. [4]Laboratory of Molecular Immunology, Immunology Frontier Research Center, Osaka University, Osaka, Japan. [5]Division of Molecular Design, Medical Institute of Bioregulation, Kyushu University, Fukuoka, Japan. [6]Division of Molecular Immunology, Medical Mycology Research Center, Chiba University, Chiba, Japan. ✉email: kshibata@yamaguchi-u.ac.jp

cancer[18]. The pathological functions and therapeutic potential of the MAIT cells remain to be elucidated.

In the present study, mass cytometry (cytometry by time of flight [CyTOF]) -based single-cell protein quantification analysis showed that, compared to healthy individuals and VKH patients in remission, the MAIT cell frequency was significantly decreased in the peripheral blood of patients with relapsing VKH who had persistent inflammation. Further, we genetically deleted MAIT cells in a mouse model of autoimmune uveitis, and found a reduction of *Il22* expression in the eye and more severe retinal pathology. After the induction of experimental autoimmune uveitis (EAU) in mice, IL-22-producing MAIT cells infiltrated the eye. In humans, reduced levels of plasma IL-22 were also more commonly observed in relapsing VKH patients compared to individuals without active ocular inflammation. Upon stimulation with the MAIT cell agonist, 5-OP-RU, human and mouse MAIT cells produced IL-22 in vitro. An intravitreal administration of 5-OP-RU to EAU mice resulted in MAIT cell expansion in the retinas, accompanied by an increased expression of *Il22* and attenuation of retinal pathology. In agreement with the protective responses, functional evaluation by electroretinography (ERG) showed improvement of visual function after the administration. These results demonstrate that metabolite-driven MAIT cell activation is a novel approach for the treatment of autoimmune uveitis.

RESULTS
MAIT cell frequency is decreased in the blood of relapsing VKH patients

VKH is a T cell-mediated, systemic autoimmune disease targeting melanocytes that are present in multiple organs including the eye, skin, inner ear, and meninges, hence, uveitogenic T cell subsets are detected in the peripheral blood of the patients[19]. To identify T cell repertoires that correlate with active VKH disease symptoms, we conducted a CyTOF-based single-cell protein quantification using peripheral blood mononuclear cells (PBMCs) on three cohorts: (1) relapsing VKH patients, (2) VKH patients under complete remission and (3) healthy donors. The data was visualized by uniform manifold approximation and projection (UMAP) non-linear dimensionality reduction[20] and then cluster frequency was quantified using a panel of established T cell subset markers[21].

In the relapsing VKH patients, systemic inflammation was characterized by a significant decrease in the non-activated naïve CD8^{+} T cell frequency compared to the healthy controls (Fig. 1a–c). In contrast, activated effector cytotoxic T cell (CTL) frequency average was increased as previously reported[22], although the increase was not significant (Fig. 1a–c).

Helper T cell subsets including Th1, Th2, Th17, Th22 and T_FH cells, which have been associated with ocular inflammation[23–25], were not significantly different between the patients with relapsing VKH and the individuals without active ocular inflammation (Fig. 1a–c). We further examined the frequency of GM-CSF-producing T (ThGM-CSF) cells in the VKH patients, since the production of GM-CSF by T cells was reported to be significantly increased in both patients with acute anterior uveitis and a mouse uveitis model[26,27]. In our patients with relapsing VKH, however, the ThGM-CSF cell frequency in PBMCs did not differ significantly from that of the subjects without active ocular inflammation (Fig. 1a–c).

Comparatively, UMAP analysis showed a cluster corresponding to MAIT cells was highly enriched in patients without active ocular inflammation but were relatively low in relapsing VKH patients (Fig. 1a, b). The frequency of MAIT cells was significantly lower in the patients with relapsing VKH than subjects without active ocular inflammation (Fig. 1c). These results were further confirmed by a flow cytometric analysis using 5-OP-RU-loaded human MR1 tetramers (hMR1/5-OP-RU-tet) as an alternative means of detecting MAIT cells (Fig. 1d). Indeed, hMR1/5-OP-RU-tet^{+} cells

expressed typical MAIT cell markers: CD161 and TRAV1-2 (Fig. 1e), and the frequency of these cells was significantly reduced in the patients with relapsing VKH (Fig. 1f). In agreement with previous studies showing that aging correlates with prognoses of VKH disease[28–30], the relapsing patients in our cohorts were all >57 years old (Fig. 1g). This result may be due to age-related decrease of MAIT cell frequencies[31] or the effect of steroid treatment[32] in the patients with relapsing VKH. These results suggest that the reduced frequencies of MAIT cells, but not other mature T cell subsets, correlate with active ocular inflammation in patients with VKH.

Uveitis is exacerbated in the absence of MAIT cells in mice

To understand MAIT cell functions in ocular inflammation, we used an EAU mouse model. After inducing EAU in wild-type (WT) mice and *Mr1*^{−/−} mice, we compared the severity of intraocular inflammation by assessing the retinal pathology as described previously[33]. In the *Mr1*^{−/−} mice, the pathological hallmarks of EAU, including retinal vasculitis and chorioretinal infiltrates, were exacerbated at day 14 after the induction of EAU and became significantly different from WT mice at day 17 (Fig. 2a, c). Supporting this, histological analysis demonstrated a greater extent of leukocyte infiltration, photoreceptor damage, and vasculitis in the *Mr1*^{−/−} mice with EAU compared to the controls (Fig. 2d; 2e, left panel).

To confirm contribution of MAIT cells to the exacerbated disease phenotype in this model, we generated mice specifically lacking MAIT cells by a homozygous deletion of *Traj33* (*Traj33*^{−/−} mice)[34] (Supplementary Fig. S1). Akin to *Mr1*^{−/−} mice, the *Traj33*^{−/−} mice with EAU presented greater severity of clinical (Fig. 2b, c) and histopathological hallmarks (Fig. 2d; 2e, right panel) compared to the WT mice with EAU. These results suggest that MAIT cells negatively regulate disease progression in this mouse model of autoimmune uveitis.

MAIT cells infiltrate the retina after EAU induction

MAIT cells in the mouse eye were analyzed using flow cytometry of single-cell suspensions from the retinas using a 5-OP-RU-loaded mouse MR1 tetramer (mMR1/5-OP-RU-tet)[14]. Almost no retinal T cells were present under normal conditions (Fig. 3a). mMR1/5-OP-RU-tet[+] TCRβ^{low} MAIT cells were detected in the WT retinas, but not in the *Traj33*^{−/−} retinas on 21 days after EAU induction (Fig. 3b, upper panels; Fig. 3d; Supplementary Fig. S2). MAIT cells were also increased in eye-draining lymph nodes between 7 and 14 days after disease induction (Fig. 3b, lower panels; Fig. 3e). The MAIT cells detected in both retinas and eye-draining lymph nodes were CD4^{−}CD8α^{−} cells (Fig. 3c), which are the most abundant population among mMR1/5-OP-RU-tet^{+} cells in the peripheral tissues of WT mice[13]. MAIT cell expansion is induced upon stimulation with their cognate antigens through their TCR[35]. After EAU induction in Nur77[GFP] mice, a faithful reporter strain used to monitor TCR stimulation[36], GFP reporter fluorescence was detected in both retinal and lymph node MAIT cells (Fig. 3f), suggesting antigenic stimulation contributes to their expansion in situ.

IL-22 is produced by MAIT cells after the induction of EAU

To determine how MAIT cells exert a protective effect against autoimmune uveitis, we analyzed the expressions of cytokines that are known to be induced by MAIT cells. MAIT cell-mediated IL-10 production has been shown to play protective roles in a mouse model of experimental autoimmune encephalomyelitis[37]. In our study, the expression of *Il10* did not decrease in the retinas of *Traj33*^{−/−} mice after EAU induction (Supplementary Fig. S3a). We also observed that *Il17a* and *Ifng*, which were shown to be involved in the pathogenesis of EAU[38], were not significantly different between the WT and *Traj33*^{−/−} retinas across all time points examined (Supplementary Fig. S3b, c). These results indicate that IL-10, IFN-γ, and IL-17A are unlikely to be induced by MAIT cells in
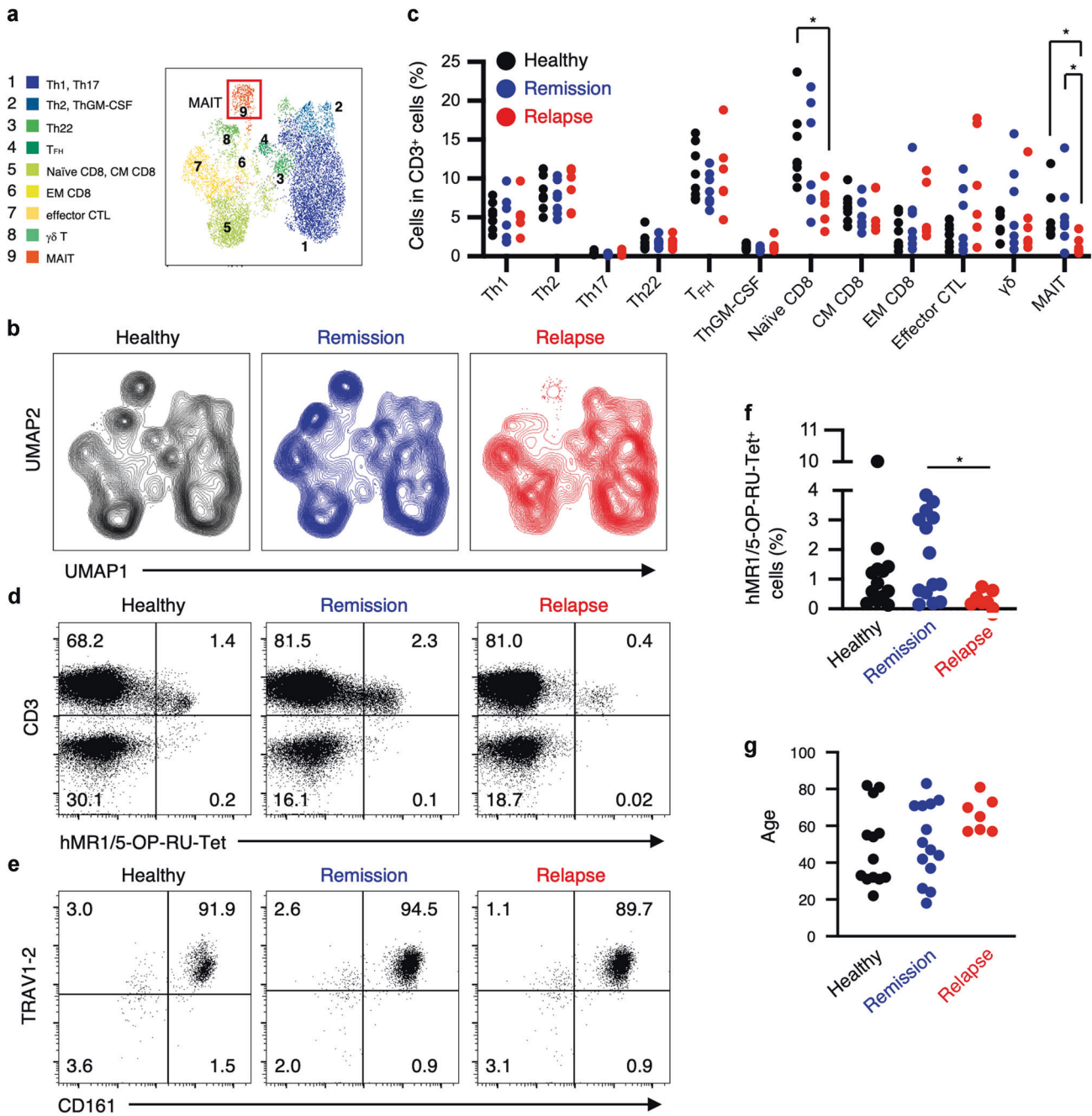
Fig. 1 The MAIT cell frequency is decreased in the relapsing VKH patients. a UMAP projections of T cell subsets in PBMCs of healthy donors by the FlowSOM clustering algorithm. MAIT cell cluster is shown in red square. **b** UMAP clusters of PBMCs from healthy donors (black), patients under remission (blue), relapsing patients (red). In each cohort, concatenated data of all individuals were used for the analysis. **c** Quantification of frequencies of T cell subsets. The percentage of each subset among CD3$^+$ cells in the peripheral blood of healthy donors ($n = 8$), VKH patients under remission ($n = 7$), and relapsing VKH patients with active inflammation ($n = 6$) is shown. Each subset was defined as follows: Th1 cells, CD4$^+$CXCR3$^+$CCR4$^-$CCR6$^-$; Th2 cells, CD4$^+$CXCR3$^-$CCR4$^-$CCR6$^-$; Th17 cells, CD4$^+$CXCR3$^-$CCR4$^-$CCR6$^+$CD161$^+$; Th22 cells, CD4$^+$CCR4$^+$CCR6$^+$CCR10$^+$; T$_{FH}$ cells, CD4$^+$CXCR5$^+$; ThGM-CSF cells, CD4$^+$CXCR3$^-$CCR4$^+$CCR6$^-$CCR10$^-$; Naïve CD8 cells, CD8$^+$CD45RA$^+$CCR7$^+$; central memory (CM) CD8 cells, CD8$^+$CD45RA$^-$CCR7$^+$; effector memory (EM) CD8 cells, CD8$^+$CD45RA$^-$CCR7$^-$; effector CTLs, CD8$^+$CD45RA$^+$CD27$^-$; γδ T cells, γδTCR$^+$; MAIT cells, TRAV1-2$^+$CD161$^+$. **d–f** Comparison of MR1-reactive T cells in the peripheral blood from the indicated populations using human MR1 tetramers loaded with 5-OP-RU (designated as 5-OP-RU-hMR1Tet$^+$ cells). Representative dot plots showing (**d**) 5-OP-RU-hMR1Tet$^+$ cells in total lymphocytes and (**e**) expressions of MAIT cell markers such as TRAV1-2 and CD161 on 5-OP-RU-hMR1Tet$^+$ cells. **f** The percentages of 5-OP-RU-Tet$^+$ cells among CD3$^+$ lymphocytes (Healthy, $n = 13$; Remission, $n = 14$; Relapse, $n = 7$). **g** The ages of individuals in three cohorts. **c, f** *$p < 0.05$ by one-way ANOVA, followed by Dunnett's multiple comparison test.

EAU, prompting us to examine other cytokines which could be responsible for the protective effect mediated by MAIT cells.

Previous reports show that IL-22 has a protective effect against EAU[39,40]. These studies motivated us to examine whether MAIT cells could produce IL-22 in our model. *Il22* expression in the retinas of WT and *Traj33*$^{-/-}$ mice were compared after EAU induction. *Il22* expression peaked after 14 days in WT retinas at significantly higher levels than that in the *Traj33*$^{-/-}$ retinas (Fig. 4a). Furthermore, intracellular staining showed that, after EAU induction, MACS-enriched retinal mMR1/5-OP-RU-tet$^+$ αβ T cells

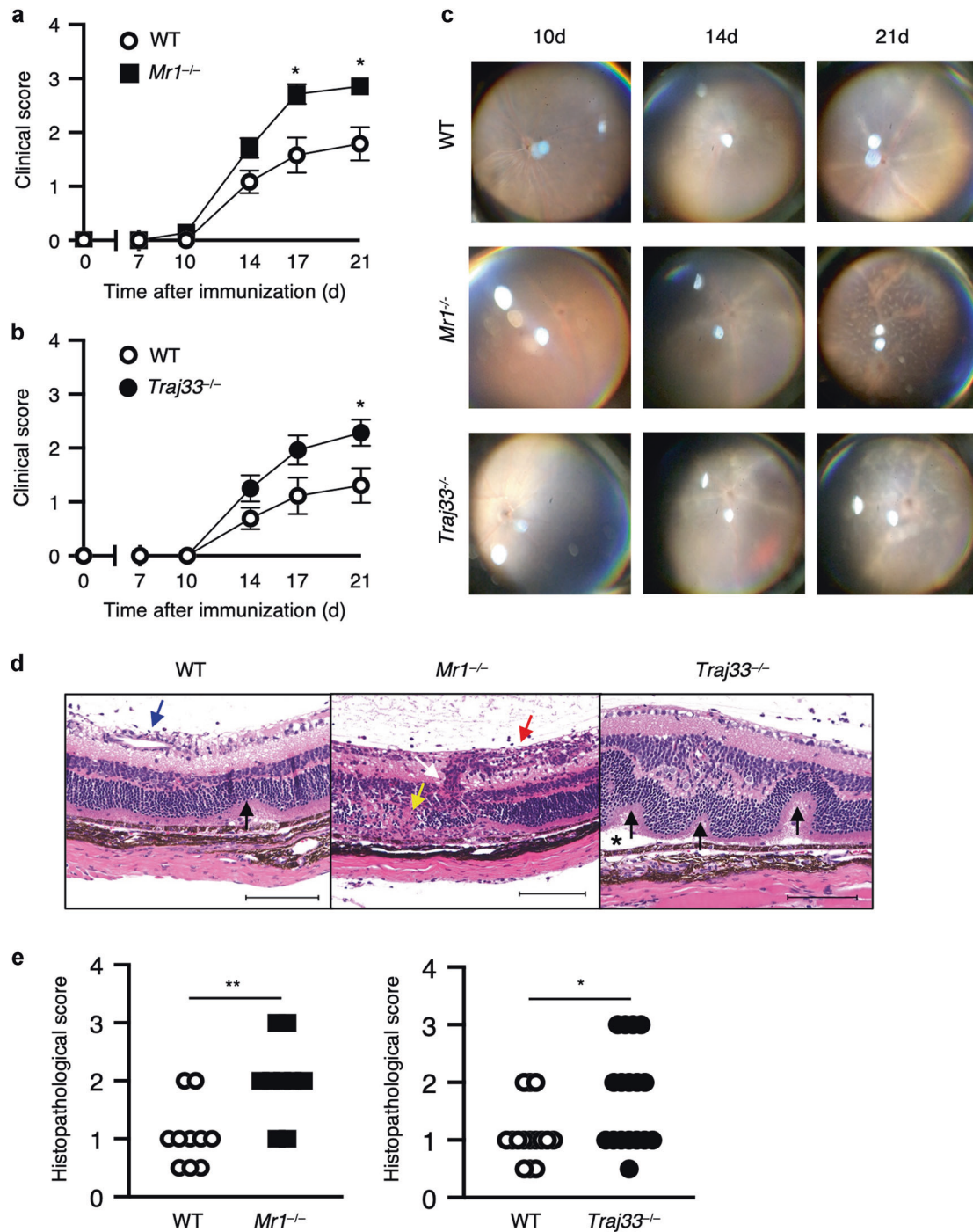**Fig. 2 MAIT cell deficiency accelerates uveitis in mice. a, b** Time course of EAU clinical scores of the indicated mice. (**a**) WT mice ($n = 12$), $Mr1^{-/-}$ mice ($n = 7$), and (**b**) WT mice ($n = 13$), $Traj33^{-/-}$ mice ($n = 14$) were used. **c** Representative retinal fundus images of the indicated mice on days 10, 14, and 21 after EAU induction. **d, e** Histopathological analysis on day 21 after EAU induction. (**d**) H&E staining of sections of eyes from indicated mice. Scale bars: 100 μm. *Arrowheads* indicate retinal folds (*black*), perivasculitis (*blue*), vasculitis (*red*), photoreceptor cell damage (*yellow*), and granulomas (*white*). An *asterisk* indicates retinal detachment. **e** The EAU histopathological scores of WT mice ($n = 15$), $Traj33^{-/-}$ mice ($n = 17$) and $Mr1^{-/-}$ mice ($n = 9$). **a, b, e** *$p < 0.05$; **$p < 0.01$ by Mann–Whitney U test. **a, b** Data are mean ± SEM. Data are representative of three independent experiments.

produced IL-22 (Fig. 4b, Supplementary Fig. S4). To confirm MAIT cell-dependent IL-22 production, we next MACS-enriched T cells from eye-draining lymph nodes of EAU-induced WT and MAIT cell-deficient $Mr1^{-/-}$ or $Traj33^{-/-}$ mice, and co-cultured these cells in the presence of antigen-presenting cells (APC). After the co-culture, IL-22 production was induced when T cells from WT mice, but not $Mr1^{-/-}$ or $Traj33^{-/-}$ mice, were used (Fig. 4c). The IL-22 production was further augmented by the addition of the MAIT cell agonist, 5-OP-RU, which was blocked by the anti-MR1 blocking antibody (Fig. 4d), suggesting that this is a partly MAIT TCR-dependent response. In addition to IL-22, TCR-dependent IL-17A production by MAIT cells was observed upon stimulation with 5-OP-RU, yet IFN-γ and IL-10 were produced to a lesser extent (Supplementary Fig. S5), consistent with the previous report[13].
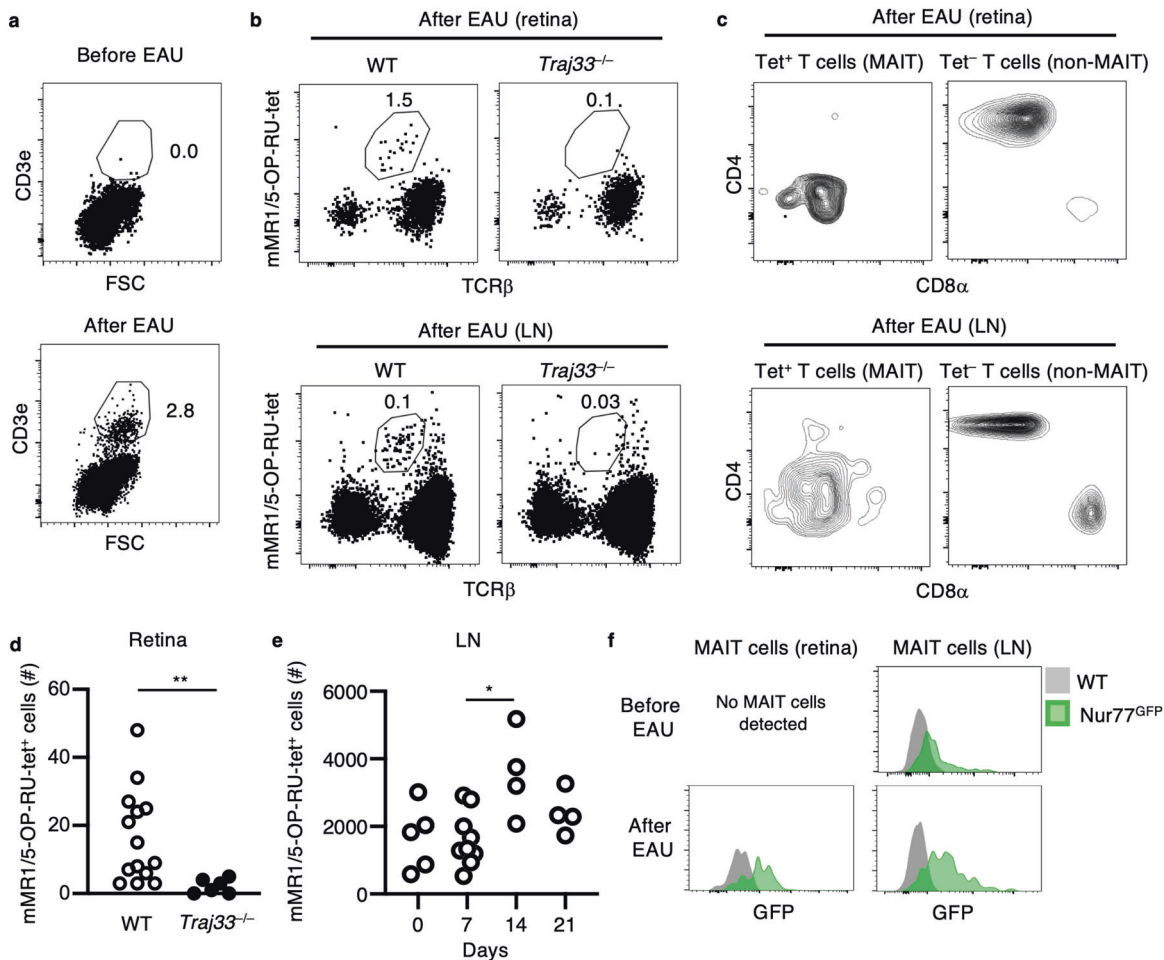
Fig. 3 **MAIT cells are infiltrated to the retina after EAU induction. a** CD3$^+$ cells in the eyes of WT mice before and after EAU induction. Numbers in the plots show CD3$^+$ cells in viable lymphocytes. **b**, **c** Flow cytometric analysis of MAIT cells from retinas (*upper panels*) and cervical lymph nodes (*lower panels*) of WT and *Traj33*$^{-/-}$ mice by using mouse MR1 tetramer loaded with 5-OP-RU (designated as mMR1/5-OP-RU-tet). Representative dot plots of (**b**) mMR1/5-OP-RU-tet$^+$ cells after gating on viable lymphocytes or (**c**) CD4 and CD8α expressions in mMR1/5-OP-RU-tet$^+$ cells. **b** Numbers in the plots indicate the percentage of mMR1/5-OP-RU-tet$^+$ cells in viable lymphocytes. The absolute numbers of mMR1/5-OP-RU-tet$^+$ cells (**d**) in the retinas of indicated mice on day 21 after EAU induction (WT, $n = 14$; *Traj33*$^{-/-}$, $n = 6$) or (**e**) in the cervical lymph nodes of WT mice at different time points after EAU induction ($n = 4$–9 at each time point). **f** GFP expressions of retinal and eye-draining lymph node mMR1/5-OP-RU-tet$^+$ MAIT cells in Nur77^{GFP} mice on day 14 after EAU induction. *$p < 0.05$, **$p < 0.01$ by (**d**) Mann–Whitney U-test or (**e**) by one-way ANOVA, followed by Dunnett's multiple comparison test. **a–c**, **f** Data are representatives of three independent experiments. **d**, **e** Data are combined from three independent experiments.

These findings suggest that, in the context of EAU, retinal MAIT cells produce IL-22 which is inducible by antigenic stimulation through their TCR.

We investigated whether the production of IL-22 could be correlated with disease symptoms in a human setting. We observed that in nine out of twenty individuals without active ocular inflammation, the concentrations of IL-22 ranged from 2 to 14 pg/mL, whereas in all seven relapsing VKH patients, the concentrations were consistently below 1 pg/mL (Fig. 4e). Similar to mouse MAIT cells, human MAIT cells produced IL-22 upon stimulation with 5-OP-RU (Fig. 4f). Taken together, these results suggest that in both mice and humans (1) the production of IL-22 is reduced when ocular inflammation is present, and (2) MAIT cells in both humans and mice produce IL-22 upon stimulation with their cognate antigen, 5-OP-RU.

The stimulation of MAIT cells by 5-OP-RU reduces retinal pathology after EAU induction

We sought to determine whether IL-22-producing MAIT cells have therapeutic potential for autoimmune uveitis. To test this, we used the MAIT cell agonist 5-OP-RU, which induced the production of

IL-22 by MAIT cells in vitro (Fig. 4d). 5-OP-RU was intravitreally administered to WT mice on day 8 after the induction of EAU (Fig. 5a). After 5-OP-RU treatment, the retinal *Il22* expression (Fig. 5b) and MAIT cell expansion (Fig. 5d) were significantly increased. Moreover, 5-OP-RU also significantly increased the expression levels of retinal *Il19* and *Ngf* which, acting in an IL-22-dependent manner, have been shown to have anti-inflammatory and neuroprotective effects, respectively[39] (Fig. 5c). 5-OP-RU treatment ameliorated pathological hallmarks of EAU, including vasculitis and retinal histopathology (Fig. 5e–h). The clinical score was enhanced by neutralization of IL-22 during the 5-OP-RU treatment (Supplementary Fig. S6), suggesting that IL-22 induced by the treatment contributes to this effect. In a complementary experiment, we performed an intravitreal injection of recombinant IL-22 (rIL-22) to WT mice with EAU. The rIL-22 treatment had a protective effect against vasculitis and retinal histopathology in EAU, similar to the 5-OP-RU treatment (Fig. 5e–h).

These results indicate that MAIT cell activation induces IL-22-mediated protective responses and attenuates disease progression in the retinas after EAU induction.
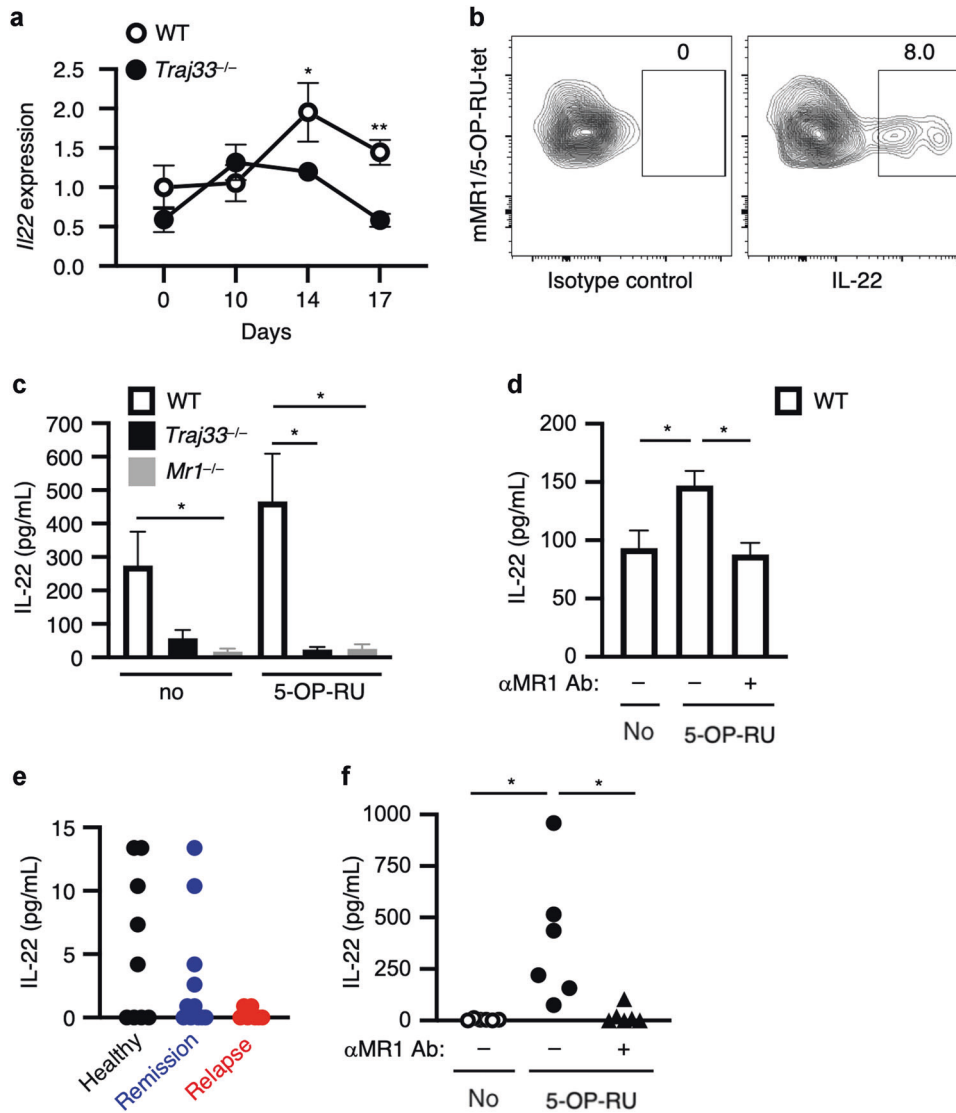
Fig. 4 MAIT cells produce IL-22. a Time-related changes of *Il22* expression in eyes after EAU induction. *Actb* expression was used as a control. WT mice ($n = 3–7$) and *Traj33*$^{-/-}$ mice ($n = 3–7$) were used at each time point. **b** IL-22 production by retinal MAIT cells pooled from 22 eyes was analyzed by intracellular staining. Numbers in the plots show the percentage of IL-22$^+$ cells in mMR1/5-OP-RU-tet$^+$ cells. **c, d** The IL-22-producing potential of MAIT cells analyzed after cultured with APCs in the presence of 5-OP-RU. On day 9 after EAU induction, αβ T cells (5×10^5 cells per well) from the indicated mice (**c** $n = 5$; **d** $n = 10$) were purified and stimulated with or without 10 μM of 5-OP-RU in the presence of mitomycin C-treated splenocytes (5×10^5 cells per well) with or without an anti- anti-MR1 blocking antibody (αMR1 Ab). At 72 h after the co-culture, the IL-22 production in the supernatants was measured by ELISA. **e** Human IL-22 productions in the sera of indicated groups (Healthy, $n = 9$; Remission, $n = 11$; Relapse, $n = 7$). **f** Human IL-22 productions of PBMCs from healthy donors after stimulation with 10 μM of 5-OP-RU in the presence or absence of an anti-MR1 blocking antibody (αMR1 Ab) ($n = 6$). **a, c, d, f** *$p < 0.05$, **$p < 0.01$ (**a**) by Mann–Whitney *U*-test or (**c, d, f**) by one-way ANOVA, followed by Dunnett's multiple comparison test. (**a, c, d**) Data are expressed as mean ± SEM. (**a, b, d, f**) Data are representatives of three independent experiments.

## MAIT cell activation partially restores visual function

To evaluate the therapeutic efficacy of 5-OP-RU administration, we performed ERG analysis[41]. This analysis allowed us to assess visual function by measuring the electrical response of retinal cells to photonic stimuli under either dark-adapted (scotopic) or light-adapted (photopic) conditions. The a-wave is produced by photoreceptors such as rods and cones, whereas the b-wave is produced by various retinal cells, including photoreceptors and neural retinal cells such as bipolar, amacrine and retinal Müller cells. After EAU induction in WT mice, clear reductions in the amplitude of both scotopic (Fig. 6a) and photopic (Fig. 6b) ERG responses were observed as compared to normal mice, suggesting that visual function was attenuated as previously described[41]. After administration of 5-OP-RU, the reduced amplitudes were

partially recovered (Fig. 6c, d). The therapeutic effect was MAIT cell-dependent as neither the recovery of visual function (Supplementary Fig. S7a–d) nor induction of *Il22* expression (Supplementary Fig. S7e) was evident after treatment with 5-OP-RU in EAU-induced *Traj33*$^{-/-}$ mice as compared with those in non-treated WT mice with EAU.

Taken together, these results suggest that MAIT cell stimulation is a potential therapeutic strategy in the treatment of autoimmune uveitis.

DISCUSSION

In the present study, we have utilized blood samples from patients relapsing with VKH and an autoimmune uveitis mouse model, to
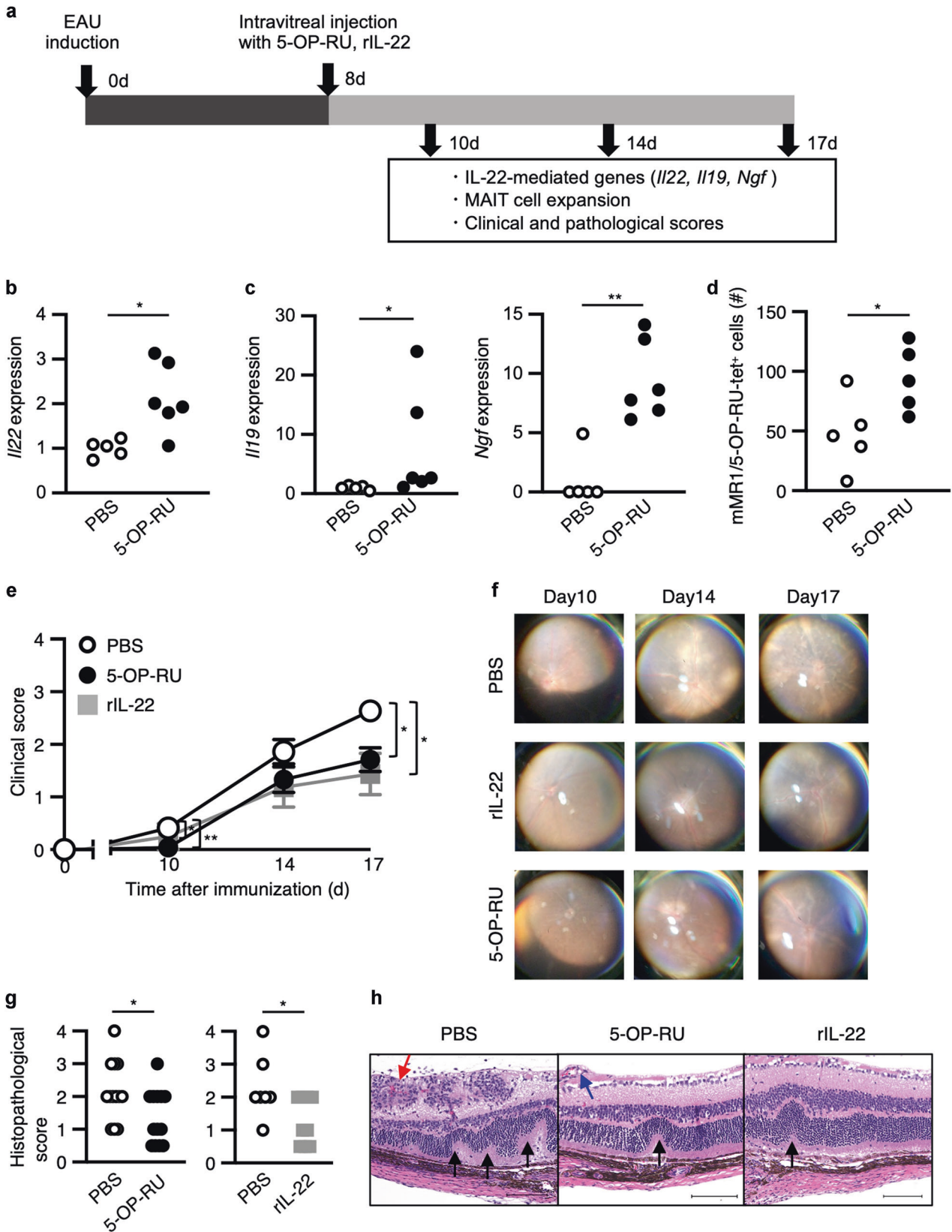
show that MAIT cells are reduced in individuals suffering from the active disease. With the use of genetic depletion of MAIT cells, and the in vivo administration of the MAIT cell agonistic metabolite, 5-OP-RU, our findings demonstrated that MAIT cells have protective roles in murine EAU. Although the protective mechanisms by MAIT cells remain to be determined, the above results indicate that metabolite-driven immunotherapy can be an alternative approach for patients with autoimmune uveitis.

Fig. 5 The activation of MAIT cells ameliorates the disease progression of EAU. a Illustration of a therapeutic strategy for the treatment of uveitis used in this study. **b** The expressions of *Il22* and (**c**) tissue repair-related genes such as *Il19* (left panel) and *Ngf* (*right panel*) in eyes on 10 days after EAU induction after treatment with 5-OP-RU or its control (PBS) are shown. The relative values to *Actb* expression are shown. **d** The MAIT cell numbers in eyes on 14 days after treatment with 5-OP-RU or its control. **e** The time course of EAU clinical scores of mice after an intravitreal administration of rIL-22 (0.33 μg/eye) and 5-OP-RU (0.84 pmol/eye) (PBS, $n = 11$; 5-OP-RU, $n = 12$; rIL-22, $n = 8$). **f** Representative retinal fundus images on day 10, 14, and 17 after immunization. **g** The histopathological EAU scores on day 17 (PBS, $n = 13$; 5-OP-RU, $n = 13$; rIL-22, $n = 9$). **h** H&E staining of sections of eyes from the indicated mice. Scale bars: 100 μm. *Arrowheads* indicate retinal folds (*black*), perivasculitis (*blue*), and vasculitis (*red*). **b–e**, **g** *$p < 0.05$, **$p < 0.01$ **e** by one-way ANOVA, followed by Dunnett's multiple comparison test or **b–d**, **g** by Mann–Whitney *U*-test. **e** Data are mean ± SEM. Data are representative of three independent experiments.

The protective functions of MAIT cells are at least in part regulated by IL-22, given our observation of (1) the dependency of *Il22* expression on the presence of MAIT cells in EAU mice (Figs. 4a), (2) the secretion of IL-22 by MAIT cells in vitro (Fig. 4b, c) and (3) the comparable protective effect of rIL-22 on EAU as shown by this study and others[39], in response to an intravitreal administration of the MAIT cell agonist (Fig. 5e–h). A previous study has shown that IL-22R expression is confined to retinal Müller cells in the eye, which in EAU, rescue the cell death of retinal ganglion cells in EAU when stimulated by IL-22[39]. Although protective effects of IL-22 on other retinal cells responsible for visual function are still unclear, IL-22 has indirect roles in protecting from visual dysfunction by inducing the expansion of regulatory T cells which suppress generation of uveitogenic T cells that target photoreceptors[39,40].

MAIT cell-dependent *Il22* expression was observed in the retinas of EAU mice, although the mechanism remains to be identified. Given that retinal MAIT cells receive TCR-mediated signals in situ (Fig. 3f), the most plausible mechanism would be that highly mobile microbiota-derived MAIT cell antigens[42] present in the eye[43] or in the intestine[44] induce the IL-22 production by MAIT cells in a TCR-dependent manner. Microbiota also activate retinal peptide-specific αβ T cells that directly cause autoimmune uveitis in mice[44]. Thus, in autoimmune uveitis, protective MAIT cell responses and pathogenic T cell responses may be facilitated by recognition of both microbial antigens. Interestingly, the composition of the gut microbiome is altered in individuals with autoimmune uveitis in both humans and mice as compared with healthy controls[45]. Thus, it is interesting to identify bacteria regulating these responses for microbiota-targeted intervention in the treatment of autoimmune uveitis as proposed recently[46].

The modulation of severity of murine EAU by MAIT cell deletion or MAIT cell activation could result from other IL-22-independent effects. It has been reported that, cutaneous MAIT cells which display a tissue repair transcriptional profile, as judged by expression of *Lgals3*, *F2r*, *Sdc1*, and *Npnt*, promote wound closure in mice with punch biopsies[47]. Likewise, upon stimulation with 5-OP-RU, human MAIT cells also induce the expression of tissue repair gene sets including *VEGFA*, *CSF1*, *THBS1* and *HIF1A*[15]. Thus, other molecules could act synergistically with IL-22 to elicit protective functions in autoimmune uveitis.

Since the identification of MAIT cell antigens[14], accumulating evidence has shown that MAIT cell frequencies are correlated with prognoses of autoimmune diseases, cancer and infection[18], although their pathological roles are not fully understood. Thus, this study provides an additional insight into understanding of unappreciated MAIT cell functions. Furthermore, as all humans express monomorphic MR1, a metabolite-driven approach for targeting MAIT cells, as proposed in this study, has the potential to become an alternative strategy for treatment of a broader range of uveitis patients which otherwise has limited therapeutic options.

METHODS
Animals
C57BL/6 mice were purchased from Kyudo. Nur77[GFP] mice (Stock# 018974) were purchased from Jackson laboratory. *Traj33*^{−/−} mice were generated

by a CRISPR-Cas9 system with C57BL/6 embryos. An Off-target analysis was performed using CRISPRdirect software (https://crispr.dbcls.jp) or CRISPRdesign software (http://crispr.mit.edu). The targeted sequence for disrupting the *Traj33* gene was shown as follows; AGCAACTATCAGTTGATCTG. *Mr1*^{−/−} mice were provided by Dr. Susan Gilfillan (Washington University in St. Louis, MO, USA). Animal study was approved by the Committee of Ethics on Animal Experiments in the Faculty of Medicine, Kyushu University. Experiments were carried out under the control of the Guidelines for Animal Experiments. Mice were treated humanely according to the ARVO Statement for the Use of Animals in Ophthalmic and Vision Research.

Induction, treatment, and evaluation of EAU
The EAU mouse model was established by immunization of co-housed 7- to 8-week-old mice with an emulsion containing human interphotoreceptor retinoid-binding protein peptide residues 1–20 (GPTHLFQPSLVLDMAKVLLD) (200 μg) in complete Freund's adjuvant (CFA) (BD Biosciences) containing 6 mg/mL *Mycobacterium tuberculosis* H37Ra. After a single intraperitoneal injection of 0.5 μg of Pertussis Toxin (Sigma), the emulsion was subcutaneously injected. In some experiments, mice were intravitreally injected with 0.84 pmol (0.28 ng) of 5-OP-RU generated from 5-amino-6-D-ribitylaminouracil (5-A-RU) (Toronto Research Chemicals) by reacting an equivalent molar ratio of methylglyoxal (Sigma) or 0.33 μg of rIL-22 (PeproTech). For IL-22 neutralization, 7 μg of an anti-mouse IL-22 monoclonal antibody (R&D systems) was used. Phosphate-buffered saline (PBS) was used as a non-treated control. The clinical score of ocular inflammation was graded on a scale of 0–4 every 3–4 days using slit-lamp microscopy and a portable camera[33,48]. For the histopathological analysis, after fixing enucleated eyes with 4% paraformaldehyde, hematoxylin and eosin staining was performed. The score of inflammation was graded on a scale of 0–4 as previous described[33].

Human studies
The study design and methods for human samples were approved by the Institutional Review Board (IRB) of The Center for Clinical and Translational Research of Kyushu University Hospital (IRB serial no. 823-043). The study was carried out in accordance with the approved guidelines. All patients or their relatives gave their informed and written consent on admission prior to their inclusion in the study. Thirteen healthy donors, fourteen VKH patients under remission, and seven relapsing VKH patients were enrolled in this study (Supplementary Table S1). Patients diagnosed based on the international criteria[49] were not selected by gender or age. The VKH patients were intravenously administered methylprednisolone 1000 mg/day for 3 days, followed by oral administration with a gradually decreased dosage of predonisolone from 32 to 48 weeks. After the treatment, the VKH patients were divided into two groups: those in remission and those with a relapse. Relapsing VKH was defined by clinical symptoms including anterior or posterior ocular inflammation over 1 year after the initiation of steroid therapy. The relapsing VKH patients enrolled in this study were not treated with biologics. PBMCs and plasma were prepared using a BD Vacutainer CPT (BD Biosciences) following the manufacturer's instructions and were stored in liquid nitrogen until use. IL-22 production in the plasma was determined using Bio-Plex Multiplex Immunoassay Kit (Bio-Rad). After 1×10^6 cells of PBMCs from healthy donors were incubated in the presence of 5-OP-RU (10 μM) with or without an anti-MR1 blocking antibody (20 μg/mL) (Biolegend) for 72 h at 37 °C, the IL-22 production in the supernatant was analyzed by a human IL-22 enzyme-linked immunosorbent assay (ELISA) kit (R&D Systems).

Flow cytometric analysis
Retinas from two eyes per individual mouse were incubated for 30 min at 37 °C in folic acid-free RPMI (Sigma) supplemented with 10% fetal calf
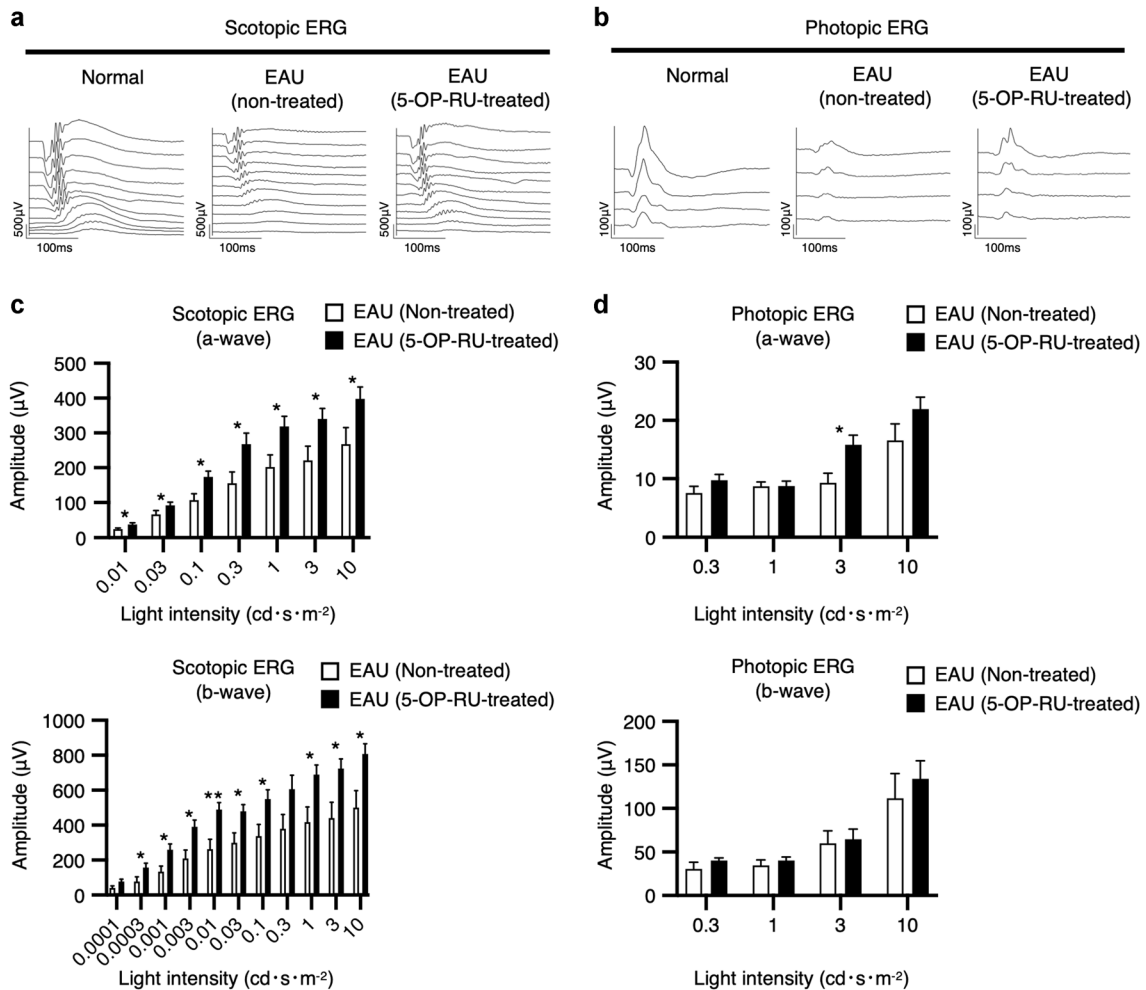
Fig. 6 Visual function is improved by treatment with 5-OP-RU. Full-field ERGs of normal WT mice, non-treated or 5-OP-RU-treated WT mice with EAU (normal WT mice, $n = 4$; non-treated WT mice with EAU, $n = 7$; 5-OP-RU-treated WT mice with EAU, $n = 7$) on 17d after EAU induction. Representative (**a**) scotopic or (**b**) photopic ERG traces in indicated mice are shown. Average amplitudes of a- (upper panels) and b- (lower panels) waves of (**c**) scotopic and (**d**) photopic ERG as in **a** and **b**. Significant difference was calculated by unpaired two-tailed Student's *t* test. *$p < 0.05$, **$p < 0.01$. **c, d** Data are mean ± SEM. The units are candela-seconds per meter squared (cd·s·m^{-2}). Data are representative of three independent experiments.

serum, 1.2 mg/mL collagenase D (Roche) and 40 µl/mL DNase 1 (Roche). After filtration through 40 µm cell strainer (FALCON), T cells were sorted by Mojosort mouse CD3 T cell Isolation kit (Biolegend) before staining. For MAIT cell enrichment, Mojosort mouse anti-PE nanobeads (Biolegend) were used. After preparation of single-cell suspensions from retinas and cervical lymph nodes, surface staining was performed by incubation for 20 min on ice. For intracellular staining, cells were stimulated with 25 ng/ml of phorbol 12-myristate 13-acetate (Sigma) and 1 µg/ml of ionomycin (Sigma) for 4 hr at 37 °C. 10 µg/ml of Brefeldin A (Sigma) was added for last 3 h. For tetramer staining, cells were incubated with tetramers for 30 min on ice prior to surface staining. 5-OP-RU-loaded mouse MR1 tetramers were provided by the NIH Core facility[14]. Human MR1 tetramers loaded with 5-OP-RU were generated using Empty human MR1 tetramer (MBL). 5-OP-RU was generated by reacting 5-A-RU (Toronto Research Chemicals) with methylglyoxal (Sigma). 5-OP-RU was added to the empty human MR1 tetramer at the concentration of 50 µg/mL. Dead cells were detected with 7-amino-actinomycin D-containing viability staining solution (Biolegend) or Zombie Aqua Fixable Viability Kit (Biolegend). Intracellular staining was performed according to the manufacturer's instruction (BD Biosciences). Stained cells were acquired with a FACS Verse (BD Biosciences) and analyzed by FlowJo ver. 10 software (BD Biosciences).

Antibodies
Antibodies used in this study were as follows: FITC-conjugated anti-mouse (m) CD3 (17A2), mTCRβ (H57-597), mCD8α (53-6.7) and anti-human (h) CD3 (UCHT1) mAbs; APC-anti-mCD4 (RM4-5), mTCRδ (GL3), mKi67 (16A8) and mIL-22 (Poly5164); PerCP/Cyanine5.5-conjugated anti-ml-A/I-E (M5/114.15.2), mCD3 (17A2), hCD19 (HIB19), hTCRδ (B1) and hCD14 (HCD14) mAbs; PECy7-conjugated-hTRAV1-2 (3C10) mAbs; BV421-conjugated mCD8α (53-6.7), mTCRβ (H57-597) and hCD161 (HP-3G10) mAbs; BV570-mCD45 (30-F11) mAb; BV650-mCD4 (RM4-5) mAb. All of the antibodies were purchased from Biolegend.

Mass cytometric analysis
First, 32 metal-conjugated antibodies were obtained from Fluidigm and Biolegend. Four antibodies obtained from Biolegend were conjugated in house using Multimetal Labeling Kits (Fludigm). Full details of the staining panel are provided in Supplementary Table S2. 1×10^6 cells per sample were initially barcoded with one or two metal-conjugated CD45 antibodies in the presence of Fc blocker for 20 min on ice and then washed in Cell Staining buffer (Fluidigm). Three cellular barcoded samples by CD45 antibodies were pooled for surface staining[50]. The cells were stained for viability with the cisplatin analog dichloro-(ethylenediamine) palladium (II) in PBS for 4 min on ice and then were stained with a metal-conjugated surface stain antibody cocktail for 30 min on ice, after which they were washed twice with the Cell Staining buffer. Cells were washed once in Cell Staining buffer and then incubated with Cell-ID Intercalator-Ir in Fix and Perm buffer (Fluidigm) for 60 min at room temperature (RT). Finally, the cells were resuspended overnight in 1.6% formaldehyde solution (Thermo Fisher Scientific). The next day, the cells were analyzed by a Helios mass

S. Yamana et al.

cytometer (Fluidigm). The data were analyzed by FlowJo ver. 10 software (BD Biosciences). The UMAP analysis was performed using 15 nearest neighbors with minimum distance of 0.5. For annotation of T cell clusters visualized by UMAP, FlowSOM analysis was performed. CD3$^+$ 3000 cells per subjects in each cohort were concatenated and 10000 cells were used for the analysis. The FlowSOM analysis was performed using 12 meta clusters. The following markers were used for these analyses: CD4, CD8, CD25, CD45RA, CD27, CD127, CD161, CCR4, CCR6, CCR7, CCR10, CXCR3, CXCR5, TRAV1-2, TCR γδ.

Real-time polymerase chain reaction

Total RNA from pooled retinas of two eyes were extracted using NucleoSpin RNA (Takara). RNA was reverse-transcribed to cDNA with a Transcriptor First Strand cDNA Synthesis kit (Roche Molecular Biochemicals). Gene expressions were semi-quantitatively analyzed by a LightCycler 96 System (Roche) using TB Green® Premix Ex Taq or MightyAmp™ for Real Time (Takara Bio). The expressions of target genes were normalized to the *Actinb* expression level. The primers used in this study were as follows: 5′-T CCAGAAGGCCCTCAGACTA-3′ and 5′-TCAGGACCAGGATCTCTTGC-3′ for *Il17a*; 5′-GTCAACCGCACCTTTATGCT-3′ and 5′-CATGTAGGGCTGGAACCTG T-3′ for *Il22*; 5′- CACGGCACAGTCATTGAAAG-3′ and 5′-GCTGATGGCCTG ATTGTCTT-3′ for *Ifng*; 5′-GCCACATGCTCCTAGAGCTG-3′ and 5′-CAGCTGGT CCTTTGTTTGAAA-3′ for *Il10*; 5′-CTCCTGGGCATGACGTTGATT-3′ and 5′-GCA TGGCTCTCTTGATCTCGT-3′ for *Il19*; 5′-TGATCGGCGTACAGGCAGA-3′ and 5′-GCTGAAGTTTAGTCCAGTGGG-3′ for *Ngf*; and 5′-GTGACGTTGACATCCGT AAAGA-3′ and 5′-GCCGGACTCATCGTACTCC-3′ for *Actinb*.

Co-culture assay for murine MAIT cells

Purified T cells from WT, $Mr1^{-/-}$ and $Traj33^{-/-}$ mice were co-cultured with mitomycin C (Nacalai tesque)-treated splenocytes for 72 h at 37 °C in the presence of 5-OP-RU (10 μM) with or without an anti-MR1 blocking antibody (20 μg/mL). Supernatants were collected and the levels of IL-22, IL-10, IL-17A, and IFN-γ were measured by mouse ELISA kits according to the manufacturer's instructions (Thermo Fisher Scientific).

Electroretinography (ERG)

After dark adaptation of mice overnight, retinal functions were evaluated by recording ERG under dim red light using PuREC (Mayo corporation). Mice were anesthetized by intraperitoneal injection of a mixture of ketamine (100 mg/kg) and xylazine (5–10 mg/kg). Mydriasis was induced with a solution combined with 0.5% tropicamide and 0.5% phenylephrine. Local anesthesia for cornea was done by treatment by eye drops of 0.4% oxybuprocaine. After these treatments, ERG was recorded for 20 min during which mice were kept warm at 37 °C. ERG was performed simultaneously in both eyes using a Ganzfeld bowl or a light emitting diode built-in contact electrodes (Mayo corporation). The contact lens electrode was placed as an active electrode on the cornea. Reference and ground electrodes were placed in the mouth and tail respectively. Responses were amplified 10,000 times and band-pass-filtered from 0.3 to 500 Hz. Scotopic ERGs were elicited with 0.3 msec flashes of white light at 1×10^{-4} to 10 cd•s•m^{-2} with appropriate delay between flashes. After bleach for 10 min, photopic ERG values were elicited by white flash at 3×10^{-1} to 10 cd•s•m^{-2} intensity.

Statistics

All statistical analyses were performed using graphing software (Prism 8; GraphPad Software). P values < 0.05 were considered significant. Statistical significance was determined by Mann–Whitney U test or unpaired two-tailed Student's t test or one-way ANOVA, followed by Dunnett's multiple comparison test.

REFERENCES

1. Gritz, D. C. & Wong, I. G. Incidence and prevalence of uveitis in Northern California; the Northern California Epidemiology of Uveitis Study. *Ophthalmology* **111**, 491–500 (2004).
2. Papotto, P. H., Marengo, E. B., Sardinha, L. R., Goldberg, A. C. & Rizzo, L. V. Immunotherapeutic strategies in autoimmune uveitis. *Autoimmun. Rev.* **13**, 909–916 (2014).
3. Caspi, R. R. A look at autoimmunity and inflammation in the eye. *J. Clin. Invest.* **120**, 3073–3083 (2010).
4. Silpa-Archa, S., Silpa-Archa, N., Preble, J. M. & Foster, C. S. Vogt-Koyanagi-Harada syndrome: perspectives for immunogenetics, multimodal imaging, and therapeutic options. *Autoimmun. Rev.* **15**, 809–819 (2016).
5. Maezawa, N., Yano, A., Taniguchi, M. & Kojima, S. The role of cytotoxic T lymphocytes in the pathogenesis of Vogt-Koyanagi-Harada disease. *Ophthalmologica* **185**, 179–186 (1982).
6. Otani, S. et al. Frequent immune response to a melanocyte specific protein KU-MEL-1 in patients with Vogt-Koyanagi-Harada disease. *Br. J. Ophthalmol.* **90**, 773–777 (2006).
7. Hsu, Y. R. et al. Noninfectious uveitis in the Asia-Pacific region. *Eye* **33**, 66–77 (2019).
8. Du, L., Kijlstra, A. & Yang, P. Vogt-Koyanagi-Harada disease: Novel insights into pathophysiology, diagnosis and treatment. *Prog. Retin. Eye Res.* **52**, 84–111 (2016).
9. Sonoda, K. H. et al. Epidemiology of uveitis in Japan: a 2016 retrospective nationwide survey. *Jpn J. Ophthalmol.* **65**, 184–190 (2021).
10. Nakayama, M., Keino, H., Watanabe, T. & Okada, A. A. Clinical features and visual outcomes of 111 patients with new-onset acute Vogt-Koyanagi-Harada disease treated with pulse intravenous corticosteroids. *Br. J. Ophthalmol.* **103**, 274–278 (2019).
11. Nishioka, Y. et al. Recurrence risk factors in patients with the Vogt-Koyanagi-Harada syndrome in Japan. *Ocul. Immunol. Inflamm.* **3**, 73–80 (1995).
12. Iwahashi, C. et al. Incidence and clinical features of recurrent Vogt-Koyanagi-Harada disease in Japanese individuals. *Jpn J. Ophthalmol.* **59**, 157–163 (2015).
13. Rahimpour, A. et al. Identification of phenotypically and functionally heterogeneous mouse mucosal-associated invariant T cells using MR1 tetramers. *J. Exp. Med.* **212**, 1095–1108 (2015).
14. Corbett, A. J. et al. T-cell activation by transitory neo-antigens derived from distinct microbial pathways. *Nature* **509**, 361–365 (2014).
15. Hinks, T. S. C. et al. Activation and in vivo evolution of the MAIT cell transcriptome in mice and humans reveals tissue repair functionality. *Cell Rep.* **28**, 3249–3262. e3245 (2019).
16. Gibbs, A. et al. MAIT cells reside in the female genital mucosa and are biased towards IL-17 and IL-22 production in response to bacterial stimulation. *Mucosal Immunol.* **10**, 35–45 (2017).
17. Rouxel, O. et al. Cytotoxic and regulatory roles of mucosal-associated invariant T cells in type 1 diabetes. *Nat. Immunol.* **18**, 1321–1331 (2017).
18. Toubal, A., Nel, I., Lotersztajn, S. & Lehuen, A. Mucosal-associated invariant T cells and disease. *Nat. Rev. Immunol.* **19**, 643–657 (2019).
19. Greco, A. et al. Vogt-Koyanagi-Harada syndrome. *Autoimmun. Rev.* **12**, 1033–1038 (2013).
20. Becht, E. et al. Dimensionality reduction for visualizing single-cell data using UMAP. *Nat. Biotechnol.* **37**, 38–44 (2019).
21. Mahnke, Y. D., Brodie, T. M., Sallusto, F., Roederer, M. & Lugli, E. The who's who of T-cell differentiation: human memory T-cell subsets. *Eur. J. Immunol.* **43**, 2797–2809 (2013).
22. Norose, K., Yano, A., Aosai, F. & Segawa, K. Immunologic analysis of cerebrospinal fluid lymphocytes in Vogt-Koyanagi-Harada disease. *Invest Ophthalmol. Vis. Sci.* **31**, 1210–1216 (1990).
23. Sugita, S. et al. Role of IL-22- and TNF-α-producing Th22 cells in uveitis patients with Behcet's disease. *J. Immunol.* **190**, 5799–5808 (2013).
24. Verhagen, F. H. et al. High-dimensional profiling reveals heterogeneity of the Th17 subset and its association with systemic immunomodulatory treatment in non-infectious uveitis. *Front. Immunol.* **9**, 2519 (2018).
25. Imai, Y. & Ohno, S. Helper T-cell subsets in uveitis. *Int. Ophthalmol. Clin.* **42**, 25–32 (2002).
26. Bing, S. J. et al. Autoimmunity to neuroretina in the concurrent absence of IFN-γ and IL-17A is mediated by a GM-CSF-driven eosinophilic inflammation. *J. Autoimmun.* **114**, 102507 (2020).
27. Huang, J. C. et al. Preliminary report on Interleukin-22, GM-CSF, and IL-17F in the pathogenesis of acute anterior uveitis. *Ocul. Immunol. Inflamm.* **27**, 1–8 (2019).
28. Chee, S. P., Jap, A. & Bacsal, K. Prognostic factors of Vogt-Koyanagi-Harada disease in Singapore. *Am. J. Ophthalmol.* **147**, 154–161.e151 (2009).
29. Kiyomoto, C. et al. Vogt-Koyanagi-Harada disease in elderly Japanese patients. *Int Ophthalmol.* **27**, 149–153 (2007).
30. Read, R. W. et al. Complications and prognostic factors in Vogt-Koyanagi-Harada disease. *Am. J. Ophthalmol.* **131**, 599–606 (2001).
31. Gherardin, N. A. et al. Human blood MAIT cell subsets defined using MR1 tetramers. *Immunol. Cell Biol.* **96**, 507–525 (2018).
32. Hinks, T. S. et al. Steroid-induced deficiency of mucosal-associated invariant T cells in the chronic obstructive pulmonary disease lung. Implications for non-typeable haemophilus influenzae infection. *Am. J. Respir. Crit. Care Med.* **194**, 1208–1218 (2016).
33. Agarwal, R. K., Silver, P. B. & Caspi, R. R. Rodent models of experimental autoimmune uveitis. *Methods Mol. Biol.* **900**, 443–469 (2012).

34. Koay, H. F. et al. Diverse MR1-restricted T cells in mice and humans. *Nat. Commun.* **10**, 2243 (2019).

35. Chen, Z. et al. Mucosal-associated invariant T-cell activation and accumulation after in vivo infection depends on microbial riboflavin synthesis and co-stimulatory signals. *Mucosal Immunol.* **10**, 58–68 (2017).

36. Moran, A. E. et al. T cell receptor signal strength in Treg and iNKT cell development demonstrated by a novel fluorescent reporter mouse. *J. Exp. Med.* **208**, 1279–1289 (2011).

37. Croxford, J. L., Miyake, S., Huang, Y. Y., Shimamura, M. & Yamamura, T. Invariant V (alpha)19i T cells regulate autoimmune inflammation. *Nat. Immunol.* **7**, 987–994 (2006).

38. Amadi-Obi, A. et al. TH17 cells contribute to uveitis and scleritis and are expanded by IL-2 and inhibited by IL-27/STAT1. *Nat. Med.* **13**, 711–718 (2007).

39. Mattapallil, M. J. et al. Interleukin 22 ameliorates neuropathology and protects from central nervous system autoimmunity. *J. Autoimmun.* **102**, 65–76 (2019).

40. Ke, Y., Sun, D., Jiang, G., Kaplan, H. J. & Shao, H. IL-22-induced regulatory CD11b+ APCs suppress experimental autoimmune uveitis. *J. Immunol.* **187**, 2130–2139 (2011).

41. Chen, J. & Caspi, R. R. Clinical and functional evaluation of ocular inflammatory disease using the model of experimental autoimmune uveitis. *Methods Mol. Biol.* **1899**, 211–227 (2019).

42. Legoux, F. et al. Microbial metabolites control the thymic development of mucosal-associated invariant T cells. *Science* **366**, 494–499 (2019).

43. St Leger, A. J. et al. An ocular commensal protects against corneal infection by driving an interleukin-17 response from mucosal γδ T cells. *Immunity* **47**, 148–158.e5 (2017).

44. Horai, R. et al. Microbiota-dependent activation of an autoreactive T cell receptor provokes autoimmunity in an immunologically privileged site. *Immunity* **43**, 343–353 (2015).

45. Ye, Z. et al. Altered gut microbiome composition in patients with Vogt-Koyanagi-Harada disease. *Gut Microbes* **11**, 539–555 (2020).

46. Salvador, R., Zhang, A., Horai, R. & Caspi, R. R. Microbiota as drivers and as therapeutic targets in ocular and tissue specific autoimmunity. *Front. Cell Dev. Biol.* **8**, 606751 (2020).

47. Constantinides, M. G. et al. MAIT cells are imprinted by the microbiota in early life and promote tissue repair. *Science* **366**, 6464 (2019).

48. Arima, M. et al. The utility of a new fundus camera using a portable slit lamp combined with a smartphone. *Acta Ophthalmol.* **97**, e814–e816 (2019).

49. Read, R. W. et al. Revised diagnostic criteria for Vogt-Koyanagi-Harada disease: report of an international committee on nomenclature. *Am. J. Ophthalmol.* **131**, 647–652 (2001).

50. Lai, L., Ong, R., Li, J. & Albani, S. A CD45-based barcoding approach to multiplex mass-cytometry (CyTOF). *Cytom. A* **87**, 369–374 (2015).

AUTHOR CONTRIBUTIONS

K.S. conceptualized the research. S.Y. performed the experiments assisted, by M.A., E.H. and S.S. K.S., S.Y., M.A., E.H., N.Y., A.T., and K.K. performed the data curation. S.Y. performed the computational analysis. K.S. and E.H. acquired funding. S.Y. provided resources. K.H.S. supervised the research. K.S. and S.Y. wrote the manuscript with input from M.A., E.H., A.T., K.K., S.Y., and K.H.S.

COMPETING INTERESTS

The authors declare no competing interests.

ADDITIONAL INFORMATION

Supplementary information The online version contains supplementary material available at https://doi.org/10.1038/s41385-021-00469-5.

Correspondence and requests for materials should be addressed to Kensuke Shibata.

Reprints and permission information is available at http://www.nature.com/reprints

Publisher's note Springer Nature remains neutral with regard to jurisdictional claims in published maps and institutional affiliations.